


Review

Mn-Based Catalysts in the Selective Reduction of NO_x with CO: Current Status, Existing Challenges, and Future Perspectives

Dianxing Lian ¹, Mohaoyang Chen ¹, Huanli Wang ¹, Chenxi Li ¹, Botao Liu ¹, Guiyao Dai ¹, Shujun Hou ¹, Yuxi Liu ^{2,*} and Yongjun Ji ^{1,*} ¹ College of Light Industry Science and Engineering, Beijing Technology and Business University, Beijing 100048, China² College of Environmental and Energy Engineering, Beijing University of Technology, Beijing 100124, China

* Correspondence: yxliu@bjut.edu.cn (Y.L.); yjji@btbu.edu.cn (Y.J.)

Abstract: The technology for the selective catalytic reduction of NO_x by CO (CO-SCR) has the capability to simultaneously eliminate CO and NO_x from industrial flue gas and automobile exhaust, thus making it a promising denitrification method. The advancement of cost-effective and high-performing catalysts is crucial for the commercialization of this technology. Mn-based catalysts demonstrate enhanced catalytic efficiency under conditions of low temperature and low oxygen content when compared to other transition metal-based catalysts, indicating significant potential for practical applications. This review outlines the diverse Mn-based catalysts, including bulk or supported MnO_x catalysts, bulk or supported Mn-based composite oxide catalysts, and the use of MnO_x as dopants. Subsequently, the synthesis methods and catalytic mechanism employed by Mn-based catalysts are presented. The following section examines the impact of O₂, H₂O, and SO₂ on the catalytic performance. Finally, the potential and implications of this reaction are deliberated. This work aims to offer theoretical guidance for the rational design of highly efficient Mn-based catalysts in the CO-SCR reaction for industrial applications.

Keywords: CO-SCR; reaction mechanism; Mn-based catalysts; O₂; H₂O; SO₂

Citation: Lian, D.; Chen, M.; Wang, H.; Li, C.; Liu, B.; Dai, G.; Hou, S.; Liu, Y.; Ji, Y. Mn-Based Catalysts in the Selective Reduction of NO_x with CO: Current Status, Existing Challenges, and Future Perspectives. *Catalysts* **2024**, *14*, 462. <https://doi.org/10.3390/catal14070462>

Academic Editors: Stefano Cimino and Rufino Navarro Yerga

Received: 31 May 2024

Revised: 10 July 2024

Accepted: 16 July 2024

Published: 18 July 2024



Copyright: © 2024 by the authors. Licensee MDPI, Basel, Switzerland. This article is an open access article distributed under the terms and conditions of the Creative Commons Attribution (CC BY) license (<https://creativecommons.org/licenses/by/4.0/>).

1. Introduction

NO_x, including NO and NO₂, constitutes a significant portion of atmospheric pollutants, which is primarily derived from vehicle exhaust and industrial emissions, notably from coke oven and coal-fired power plant emissions. NO_x can cause severe environmental consequences, such as acid rain, photochemical smog, and ozone depletion [1–3], which present substantial hazards to human health. Currently, the prevalent industrial denitrification technique involves the selective reduction of NO_x by NH₃, known as NH₃-SCR [4,5]. However, this technology presents several concerns, including the potential for ammonia storage leakage, the formation of by-products that can lead to equipment blockage and corrosion, and the inherent toxicity of ammonia [6]. Given the incomplete combustion of fuel, flue gas also contains a certain amount of CO. The use of CO as the reducing agents for the selective catalytic reduction of NO_x (CO-SCR) obviates the necessity for extra reducing agents, thereby reducing costs. Moreover, this technology assists in the removal of NO_x and CO emissions, enabling the concurrent elimination of both pollutants. Hence, CO-SCR technology shows promising potential for practical application [7].

The ideal CO-SCR reaction is presented in Equation (1). However, in real flue gas, there exists a high concentration of O₂ and H₂O, along with a minor quantity of SO₂. The presence of oxygen can lead to the preferential oxidation of NO and CO (Equations (2) and (3)), while the existence of H₂O and SO₂ may cause catalyst poisoning; meanwhile, concurrent side reactions may occur, producing N₂O (Equation (4)), consequently diminishing the selectivity for N₂.





Currently, the catalysts employed for the CO-SCR reaction are predominantly categorized into two groups: noble metal catalysts and transition metal catalysts. Noble metal catalysts, such as those based on Pd [8], Pt [9], and Ir [10], offer certain benefits such as resistance to oxygen and high temperatures. However, some challenges exist, such as the scarcity of precious metal, elevated costs, high reduction temperatures, and susceptibility to sulfur- and water-induced deactivation [11]. For instance, in three-way catalyst (TWC) systems, the CO-SCR reaction occurs concurrently with other reactions in the exhaust pipe of a vehicle, which operates at high temperatures and low oxygen concentrations. In this instance, the typical catalyst comprises Pt, Pd, and Rh. In contrast, transition metal catalysts like Co-based [12], Mn-based [13], Cu-based [14] ones are preferred due to their lower cost and superior catalytic activity at lower temperatures compared to noble metal catalysts. Therefore, employing transition metal catalysts in CO-SCR is a favorable approach. Nevertheless, in oxygen-rich environments, transition metals tend to be oxidized easily, leading to diminished oxygen resistance, N₂ selectivity, and stability. Therefore, it is imperative to develop cost-effective and efficient transition metal catalysts, which should exhibit low-temperature catalytic reactivity, a broad temperature range, high O₂ tolerance, resilience to SO₂ and H₂O poisoning, and long-lasting stability.

In prior reviews, researchers have provided a summary of catalysts based on Ir [15], Cu [16,17], and various transition metals [18]. Additionally, they have categorized and deliberated on various noble catalyst types [19–21]. It is known that Mn-based catalysts exhibit multiple oxidation states (Mn²⁺, Mn³⁺, and Mn⁴⁺), excellent redox capacity, and abundant reactive oxygen species. Furthermore, Mn has the capability to be integrated into various functional materials. More importantly, Mn-based catalysts have demonstrated superior performances at low temperatures compared to other transition metal catalysts, showing promising potential for use in the CO-SCR reaction. Thus, in recent years, Mn-based catalysts have garnered increasing attention. However, they still encounter issues related to inadequate oxygen resistance and instability. Given the scarcity of literature reviews dedicated to Mn-based catalysts in the CO-SCR reaction, this review provides a comprehensive examination of Mn-based catalysts, in terms of their current status, existing challenges, and future perspectives, aiming to facilitate their industrial applications.

As illustrated in Figure 1, this review commences with an exploration of the various classifications of Mn-based catalysts, followed by an examination of the synthesis methods and a discussion of the reaction mechanism. It also offers a summary of the impact of O₂, H₂O, and SO₂ on the catalytic efficiency of Mn-based catalysts. This discussion is followed by an examination of the challenges faced by these catalysts and the strategies developed to address them. Finally, this review concludes by suggesting innovative strategies for the advancement of highly effective Mn-based catalysts to enhance their future prospects.

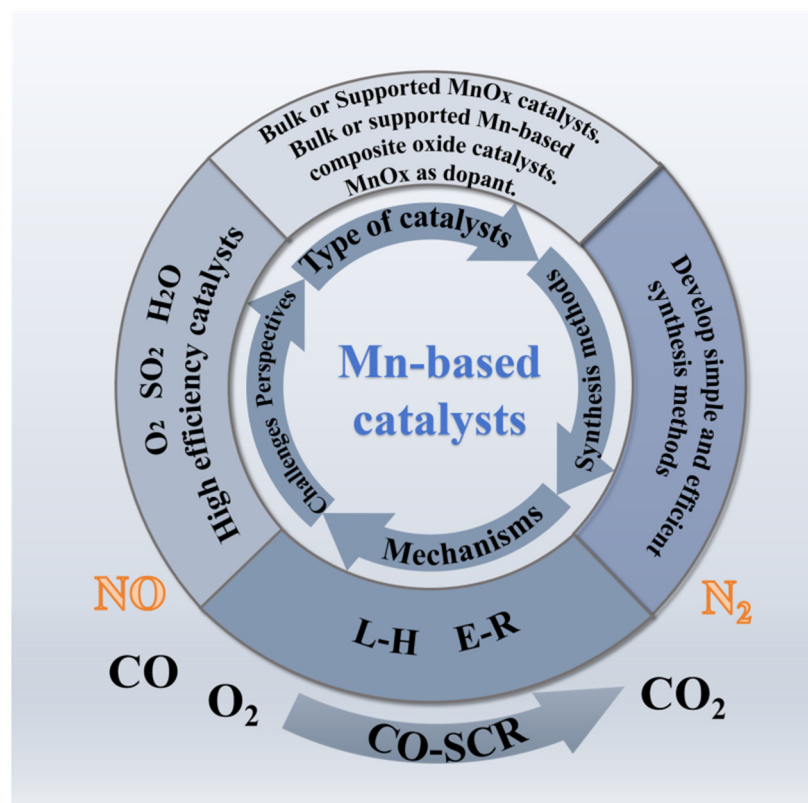


Figure 1. An overview of Mn-based catalysts.

2. Types of Mn-Based Catalysts

2.1. Bulk or Supported MnO_x Catalysts

Manganese oxides, which are present in various crystal phases, are compounds characterized by multiple oxidation states (Mn^{2+} , Mn^{3+} , and Mn^{4+}), excellent redox capabilities, and a rich supply of active oxygen. The efficiency of pure manganese oxides in reducing NO_x to N_2 is ranked $MnO_2 > Mn_5O_8 > Mn_2O_3 > Mn_3O_4 > MnO$. Highly oxidized manganese oxides have higher CO-SCR activity, and oxygen vacancies (OVs) produced in the reduction process serve as the adsorption site for NO_x [22]. These properties empower them to actively engage in and promote catalytic reactions. Therefore, manganese oxides hold great potential in the CO-SCR reaction (Table 1). The surface manganese oxide phases and redox properties of Mn oxide catalysts are crucial factors that significantly influence the overall catalytic activity [23]. For the α - MnO_2 nanorod catalyst, upon pretreatment with H_2 , Mn^{4+} is first reduced to Mn^{2+} . Subsequently, these Mn^{2+} sites undergo rapid oxidation to Mn^{3+} in the presence of NO . In situ studies showed that the α - MnO_2 surface experiences significant recombination, forming a new surface active phase. Mn^{3+} and OVs were the active sites [24].

Compared with other transition metal oxides, the low temperature activity of manganese oxides on support for CO-SCR is higher than that of other transition metal oxides. Boningari et al. [25] studied different titanium-supported transition metal-based catalysts and found that MnO_x/TiO_2 had better CO-SCR performance at low temperatures. In situ infrared spectroscopy showed that the Lewis acid site on the catalyst surface was responsible for the reaction, not the Brønsted acid site. The reduced Mn site served as the active site for activating NO . In Mn/TiO_2 catalysts, the lattice oxygen proximal to Mn atoms facilitates the oxidation of CO to CO_2 , leading to the creation of OVs. On Mn/TiO_2 , the notable intermediate N_2O can be reduced to N_2 , with an associated energy barrier of 0.51 eV, indicating a pronounced N_2 selectivity. The Mn–OV pair present on the catalyst surface serves as the active site for the adsorption of NO and the catalysis of N–O bond cleavage [26]. Moreover, the comparison of the activities of different transition metal oxides

(Cu, Ni, Fe, Mn, and Cr) showed that the TiO₂-supported manganese oxide has good NO reduction activity at 200 °C. The MnO_x/TiO₂ catalyst showed highly N₂ selectivity even in the presence of oxygen. The results indicate that the high surface area and the reducibility of manganese oxide play an important role in the high activity for CO-SCR [27].

Table 1. Comparison of catalytic performances of the Mn-based catalysts in the literature.

Catalyst	Gas Composition (%)					GHSV or WHSV	Temperature (°C)	NO Conversion (%)	CO Conversion (%)	N ₂ Selectivity (%)	Ref.
	NO	CO	O ₂	SO ₂	H ₂ O						
α-MnO ₂ nanorods	5.0	5.0	---	---	---	30,000 mL h ⁻¹ g ⁻¹	400	85	---	80	[24]
MnO ₂ /TiO ₂	0.4	0.4	2.0	---	---	50,000 h ⁻¹	200	95	---	---	[25]
Mn/TiO ₂	3.0	3.0	---	---	---	20,000 h ⁻¹	450	100	---	90	[26]
MnO _x /TiO ₂	0.4	0.4	2.0	---	---	50,000 h ⁻¹	175	100	---	100	[27]
2MnO _x -Fe ₃ O ₄	1.0	2.0	---	---	---	23,000 h ⁻¹	400	90	---	70	[28]
Cu _{1.5} Mn _{1.5} O ₄	5.0	10.0	---	---	---	24,000 mL h ⁻¹ g ⁻¹	250	100	45	95	[29]
CuO-Mn ₂ O ₃ /γ-Al ₂ O ₃	5.0	10.0	---	---	---	24,000 h ⁻¹	300	70	---	85	[30]
NiMn-MOF-74	0.5	1.0	---	0.1	5.0	30,000 h ⁻¹	200	100	---	---	[31]
Co _{0.3} -OMS-2	0.5	0.5	---	1.0	---	24,000 mL h ⁻¹ g ⁻¹	150	95	---	80	[32]
Cu _x Mn _{3-x} O ₄	1.0	2.0	---	---	---	30,000 h ⁻¹	200	100	---	55	[33]
Cu-Ce-Fe-Mn/TiO ₂	0.02	0.02	1.0	---	---	10,000 h ⁻¹	200	100	82	---	[34]
0.010 _{MnFeCu}	5.0	10.0	---	1.0	10.0	15,000 mL h ⁻¹ g ⁻¹	300	100	---	100	[35]
Mn@La ₃ -Fe ₁ /AC	0.25	5.0	10.0	---	---	26,000 h ⁻¹	400	93.8	---	---	[36]
Mn _x Co _{3-x} O ₄	1.0	2.0	5.0	0.05	5.0	20,000 h ⁻¹	180	100	---	100	[37]
Mn-CeO ₂ @Co ₃ O ₄	1.0	2.0	5.0	0.05	10.0	24,000 h ⁻¹	200	82	100	78	[38]
Cu-Mn ₂	0.6	1.6	5.0	---	---	15,000 h ⁻¹	400	90	100	87	[39]
CuMnO ₂	1.0	2.0	---	---	---	13,000 h ⁻¹	300	100	---	80	[40]
V _x -OMS-2	0.5	0.5	---	1.0	---	24,000 mL h ⁻¹ g ⁻¹	300	95	---	---	[41]
Sb _{0.2} -OMS-2	0.05	0.05	---	---	---	---	300	100	90	---	[42]
Ho _x -OMS-2	0.05	0.05	0.05	---	---	15,000 h ⁻¹	225	100	99	---	[43]

2.2. Bulk or Supported Mn-Based Composite Oxide Catalysts

When Mn forms a composite oxide with other metals, it frequently generates a synergistic effect, enhancing its catalytic performance beyond that of an individual Mn oxide (Table 1) [28]. The presence of surface synergistic oxygen vacancies (SSOVs) within composite oxides facilitates the adsorption and activation of gas molecules, thereby enhancing catalytic performance. In comparison to pure MnO_x, Cu-Mn catalysts demonstrate a higher propensity for oxidation and the generation of activated O species on their surface, thus promoting the adsorption of oxygen molecules. Mn-based catalysts doped with copper oxide comprise not only MnO_x but also a linear Cu-CO active substance, which enhances the adsorption of NO_x. An intriguing phenomenon is that the surface dispersed Cu^{x+}-O²⁻-Mn^{y+} substance can be reduced to Cu⁺-□-Mn^{(4-x)+} active species with an elevation in adsorption temperature. The synergistic effect between Cu and Mn (Cu^{x+}-O²⁻-Mn^{y+}) plays a crucial role in the CO-SCR reaction (Figure 2a) [29]. Yao et al. [44] synthesized CuO-MnO₂/CeO₂ using the co-impregnation method, which exhibited a stronger interaction and an excellent reduction behavior. This process facilitated the generation of low-valence copper species (Cu⁺/Cu⁰) and increased oxygen vacancies, particularly SSOVs (Cu⁺-□-Mn^{(4-x)+}), during the reaction, which are conducive to the adsorption of CO and the dissociation of NO, respectively. In another study [30], it was found that the catalytic efficiency of CuO-Mn₂O₃/γ-Al₂O₃ catalysts, after being pretreated with CO, exhibited superior performance compared to CuO/γ-Al₂O₃ and Mn₂O₃/γ-Al₂O₃. The formation of SSOVs in the CuO-Mn₂O₃/γ-Al₂O₃ catalyst occurs following CO pretreatment, leading to distinct adsorption properties compared to SOVs in CuO/γ-Al₂O₃ and Mn₂O₃/γ-Al₂O₃ catalysts. Exposed Cu⁺ and Mn²⁺ ions act synergistically as CO and NO adsorption sites, respectively, and the SSOVs function as a crucial bridge, facilitating the interaction between adjacent adsorbed CO and NO to promote the surface reaction. Therefore, SSOVs on the CO-CuMnAl catalyst exhibit superior catalytic activity, facilitating the reduction of NO by CO (Figure 2b) [30]. Due to the difference in cation radius, the incorporation of Mn and

Ni into MOF-74 leads to an improvement in the specific surface area, which is conducive to the formation of unsaturated coordination metal sites and Lewis acid sites for CO-SCR. In addition, the electron interaction between Ni and Mn in NiMn-MOF-74 facilitates a significant synergistic reaction ($\text{Mn}^{3+} + \text{Ni}^{3+} \leftrightarrow \text{Mn}^{4+} + \text{Ni}^{2+}$). This synergistic effect not only enhances the formation of more active Mn^{4+} components, but also promotes the generation of SSOVs, which exhibit higher catalytic activity compared to surface oxygen vacancies (SOVs) [31].

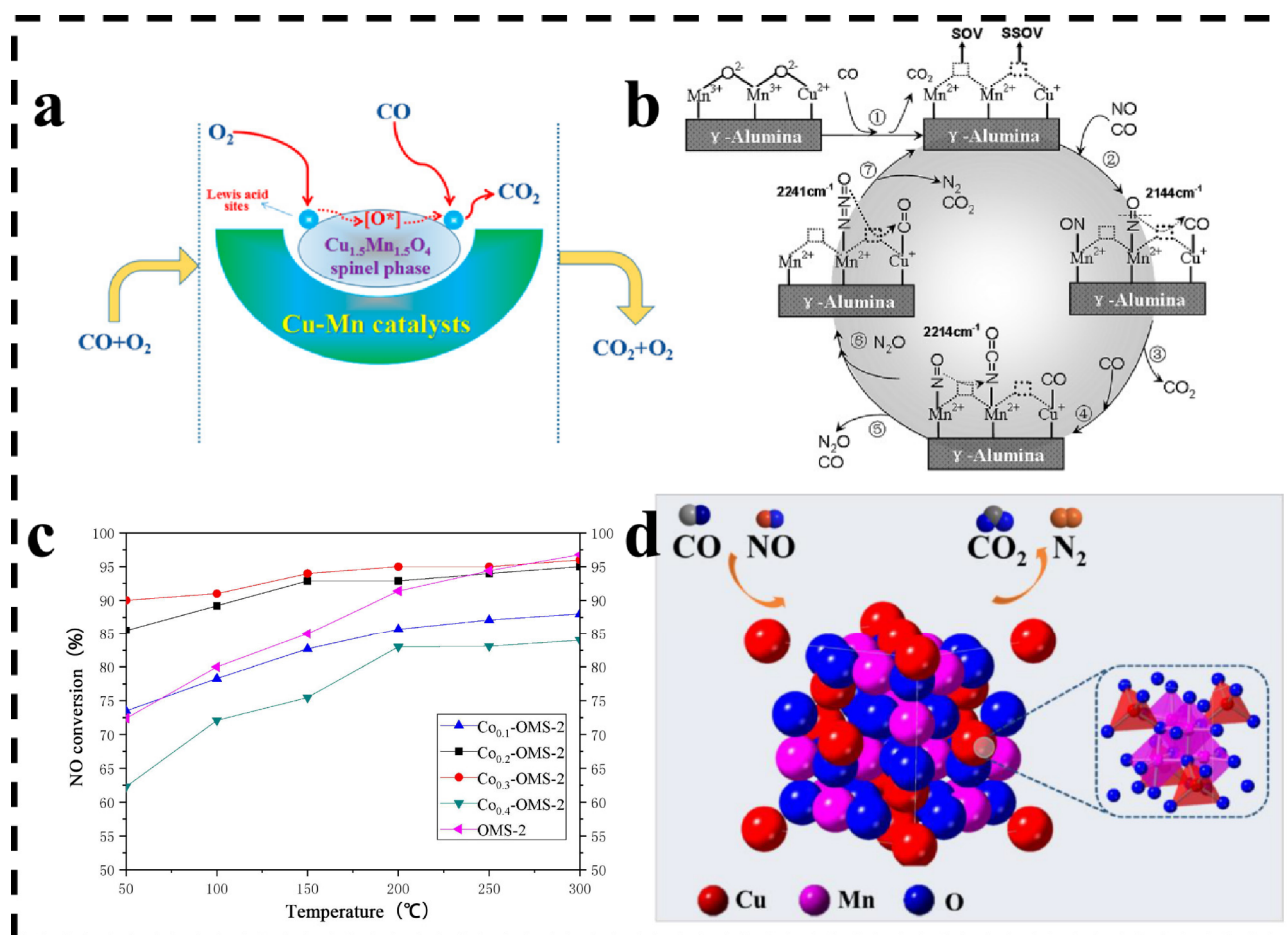


Figure 2. (a) Schematic illustration of the proposed mechanism for the catalytic oxidation of CO over Cu–Mn catalysts [29]; (b) proposed reaction mechanism for NO reduction by CO over CO–CuMnAl catalyst [30]; (c) NO conversion curves of OMS–2 prepared by Co doping method [32]; (d) schematic illustration of the proposed mechanism for the catalytic CO-SCR over $\text{Cu}_x\text{Mn}_{3-x}\text{O}_4$ catalysts [33].

By adjusting the electronic configuration of manganese oxides, it is possible to alter their redox characteristics, subsequently impacting their catalytic efficiency. During the doping modification process, Co occupies the Mn site in the $[\text{MnO}_6]$ cell in the OMS-2 catalyst, forming a new $[\text{CoO}_6]$ crystal structure. The crystallinity of Co-doped OMS-2 decreases as the Co doping amount increases. Co substitutes for Mn, creating a novel active site. The active sites comprising Co^{2+} , Co^{3+} , Mn^{3+} , and Mn^{4+} adsorb CO and NO, catalyzing the conversion of these compounds into CO_2 and N_2 (Equations (9) and (10)). Compared with undoped OMS-2, the conversion of NO in the flue gas of $\text{Co}_{0.3}$ -OMS-2 reaches approximately 95% at 100–300 $^{\circ}\text{C}$ (Figure 2c) [32]. In the case of the $\text{Cu}_x\text{Mn}_{3-x}\text{O}_4$ catalyst, the introduction of copper ions into Mn_2O_3 results in the formation of a spinel structure with a high density of lattice defects and oxygen vacancies. This modification increases the concentration of Mn^{4+} , which has the capability to adsorb reactant molecules. Consequently, this process enhances the redox performance of the catalyst, increases the

mobility of reactive oxygen species, and ultimately boosts its catalytic activity. Compared with CuO and Mn₂O₃, the catalytic activity of the Cu_xMn_{3-x}O₄ catalyst is enhanced. The strong synergy between binary metal oxides also results in its improved stability (Figure 2d) [33]. Mn demonstrates a propensity to exhibit synergistic interactions with other metals, resulting in increased efficacy of catalysts operating at low temperatures. When Ce, Fe and Co were introduced into a Mn-based catalyst and supported on TiO₂, the catalytic performance exhibited an enhancement compared to the performance of Mn alone. Under anaerobic conditions, the Mn-Ce-Fe-Co/TiO₂ catalyst achieved complete NO conversion at 200 °C. The enhanced performance of the modified Mn-based catalyst can be attributed to the increased oxygen mobility and the formation of Mn⁴⁺, resulting in an elevated rate of NO conversion [34].

2.3. MnO_x as Dopants

Mn is also a frequently utilized dopant in CO-SCR (Table 1). The introduction of Mn doping has been found to facilitate the generation of oxygen vacancies on the catalyst surface. This, in turn, enhances the adsorption and activation of NO, leading to an overall improvement in the catalyst's performance. When Cu²⁺ and Fe³⁺ combine to form a Fe-based composite oxide in an alkaline solution, the addition of a specific quantity of Mn facilitates its bonding with Fe. This process weakens the interaction between Cu and Fe, leading to the precipitation of the CuO phase. The Cu²⁺ ions then selectively develop along the surface of CuO(110), leading to enhanced catalytic activity. At high temperatures (300–1000 °C), the presence of Mn³⁺ can impede the conversion of γ-Fe₂O₃ to α-Fe₂O₃, thus achieving stable catalytic efficacy. The existence of Mn⁴⁺ leads to the generation of reactive oxygen species, which can be readily reduced to create SSOVs during the reaction. The resulting SSOVs can promote the dissociation of NO and facilitate the oxygen transfer (Equation (5)). These factors ultimately result in the catalyst exhibiting good catalytic performance across a wide temperature range [35]. Different metal cations M (M = Zr, Cr, Mn, Fe, Co, and Sn) were doped into a CuO/Ce₂₀M₁O_x catalyst to explore their impact on the catalyst's structure and activity in the CO-SCR reaction. It was found that the doping of Mn⁴⁺ into the CeO₂ lattice promoted the generation of oxygen vacancies and surface unsaturated metal cation. Hence, in comparison to Cu/CeO₂ and other metal cation-doped samples, Cu/CeMnO_x demonstrated superior performance [45]. When MnO_x was doped into CuCeO_x/γ-Al₂O₃, it significantly enhanced the catalytic activity at low temperatures, with maximum conversions of NO_x and CO of 98% and 96%, respectively, at 200 °C. The robust interaction among Mn, Cu, and Ce oxides results in higher dispersibility and more coordination-unsaturated ions. In addition, this interaction enhances the formation of oxygen vacancies and acid sites, thereby enhancing the adsorption capacity for CO and NO_x [36]. The rise in the Fe²⁺/Fe³⁺ ratio subsequent to the addition of an accelerant to the La-Fe/AC catalyst could be attributed to the supplementary synergistic impact of M (Mn and Ce) and Fe via the redox equilibrium (M³⁺ + Fe³⁺ ↔ M⁴⁺ + Fe²⁺). This phenomenon improves the redox cycle, promotes the formation of SSOVs, aids in the decomposition of NO, and accelerates the CO-SCR process. The presence of O₂ promotes the formation of C(O) complexes and enhances the activation of metal sites. The NO conversion of a Mn@La₃-Fe₁/AC catalyst reached 93.8% at 400 °C with 10% O₂ [37]. Our group reported that the hierarchically interconnected porous (HIP) Mn_xCo_{3-x}O₄ spinel, synthesized through a citric acid-assisted sol-gel method, demonstrated high catalytic efficiency for CO-SCR. The NO removal efficiency of the synthesized Mn_{0.3}Co_{2.7}O₄ was 87% at 180 °C, exhibiting a wide active temperature range (100–400 °C). Its superior activity can be attributed to the following factors: (i) the high oxidation states of Mn³⁺, Mn⁴⁺, and Co³⁺ in the Co-O-Mn structure facilitates an effective redox cycle, creating adsorption sites for NO and CO (Equations (9) and (10)), and (ii) the HIP structure significantly enhances gas diffusion (Figure 3a) [46].

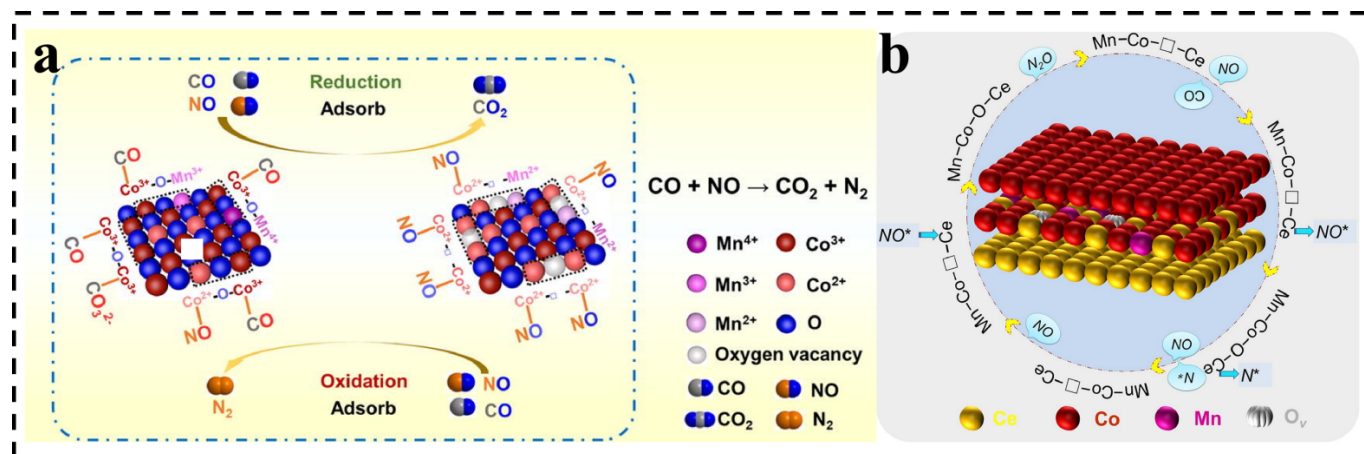


Figure 3. (a) Schematic illustration of proposed CO-SCR reaction mechanism on $\text{Mn}_{0.3}\text{Co}_{2.7}\text{O}_4$ [46]; (b) schematic illustration of proposed CO-SCR reaction mechanism on $\text{Mn}-\text{CeO}_2@\text{Co}_3\text{O}_4$ [38].

Moreover, the catalyst's electronic structure can be modified through Mn doping to enhance its catalytic performance. Doping Mn into $\text{CeO}_2@\text{Co}_3\text{O}_4$ generates additional active sites and modulates the electronic structure of the catalyst (Figure 3b). When the O_2 concentration was 5 vol% and the temperature was 200 °C, the $\text{Mn}-\text{CeO}_2@\text{Co}_3\text{O}_4$ catalyst exhibited an NO conversion of 82%, a CO conversion of 100%, and an N_2 selectivity of 78% [38]. In the Mn_2O_3 -modified $\text{CuO}/\gamma\text{-Al}_2\text{O}_3$ catalyst prepared by Wan et al. [47], it was found that Mn_2O_3 can promote the dispersion of CuO on $\gamma\text{-Al}_2\text{O}_3$, forming a monomolecular layer. This enhances the reducibility of CuO ($\text{Cu}^{2+} + \text{Mn}^{3+} \leftrightarrow \text{Cu}^+ + \text{Mn}^{4+}$), thus boosting the adsorption capacity of CO on the $\text{CuO}/\gamma\text{-Al}_2\text{O}_3$ catalyst (Equation (9)). As a result, both NO conversion and N_2 selectivity are enhanced.

3. Synthesis Methods

Various synthesis methods yield distinct structures, influencing factors like the particle size, the creation of specific morphologies, the generation of OVVs, or the regulation of valence states of the active center. These factors, in turn, impact the catalytic activity [39].

In order to implement the catalyst in industrial settings, it is imperative to devise a synthesis approach that is easy to execute, amenable to upscaling, and cost-effective. Currently, alternative preparation methods distinct from conventional synthesis techniques have been reported in the literature. For instance, smooth spherical $\text{Fe}_x\text{Mn}_y\text{O}$ catalysts with varying Fe contents were synthesized using the solvothermal method, and their CO-SCR activity was tested. The results indicated that the introduction of FeO_x enhances the $\text{Fe}^{2+} + \text{Mn}^{4+} \leftrightarrow \text{Fe}^{3+} + \text{Mn}^{3+}$ conversion, thereby facilitating oxygen cavitation and the production of reactive oxygen species [40]. Also, a series of spherical $\text{Mn}_x\text{-Fe}_2\text{O}_3/\text{C}$ catalysts were synthesized using MnFe-MOF-74 as a precursor through the sacrif-membrane plate method, and they were used in the CO-SCR process. The characterization results revealed the formation of a redox reaction involving Fe^{2+} and Mn^{4+} ions at the Fe-O-Mn site, leading to the generation of $\text{Fe}^{3+} + \text{Mn}^{3+}$ ions. This reaction significantly enhanced the adsorption and activation of NO molecules. DFT calculations revealed that the incorporation of Mn substantially enhances the local electron density at Fe-Mn sites, resulting not only in the formation of robust C-Fe/Mn and N-Fe/Mn bonds, but also in the effective weakening of N-O bonds [48]. While these approaches enhance the catalytic performance of Mn-based catalysts in the CO-SCR reaction, they are associated with complex operational procedures and high expenses.

Several researchers have employed coprecipitation as a method to synthesize La-Cu-Mn-O catalysts with varying La concentrations. The incorporation of La has been shown to facilitate the diminution of the particle size of copper-manganese oxides, inhibit its agglomeration, improve the reducibility of the catalyst, and stimulate the augmentation

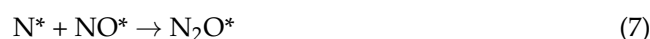
of the exposed active sites and the reactivity between the reactants (NO and CO) [49]. Although the co-precipitation method is straightforward, the utilization of La is cost-prohibitive, rendering it impractical for industrial applications.

Due to the complexity or high cost associated with the current synthesis methods, there is a need to establish a straightforward and effective synthesis approach that achieves catalytic activity for the preparation of the catalyst.

4. Reaction Mechanism

Generally, there exist three mechanisms for the CO-SCR reaction. The mechanisms are categorized into the Langmuir–Hinshelwood (L-H) mechanism, the Eley–Rideal (E–R) mechanism, and the Mars–Van Krevelen (MvK) mechanism. The L-H mechanism involves the adsorption of two reaction gas molecules on the catalyst's surface, where the reaction proceeds through the interactions between the adsorbed species [50–52]. In contrast, the E-R mechanism entails the adsorption of a reactant gas on the catalyst's surface, with the reaction occurring through molecular interactions between the adsorbed species and the gas-phase molecules [53–55]. The MvK mechanism primarily pertains to reactions that involve active lattice oxygen [50,56,57]. For Mn-based catalysts, many studies have identified the prevalent mechanisms governing the CO-SCR reaction as the L-H mechanism [31,33,38,58] and the E-R mechanism [23–25,49]. To date, there is no literature reporting the involvement of the MvK mechanism in the CO-SCR reaction, where N₂O acts as the principal reaction intermediate in this process.

The E-R mechanism is likely to occur when Mn predominantly exists in a low valence state in Mn-based catalysts. For the E-R mechanism, the formation of N₂O can be described as follows: NO initially adsorbs on the catalyst to produce NO* (Equation (5)). Subsequently, NO* dissociates into N* and O* (Equation (6)), and N* reacts with another adsorbed NO to form N₂O* (Equation (7)). Finally, the adsorbed N₂O is reduced to N₂ and CO₂ by gaseous CO (Equation (8), where * denotes the adsorbed state).



The E-R mechanism is more likely to occur at low temperatures. Shan et al. [24] synthesized α -MnO₂ nanorods using a colloidal method and studied their catalytic behavior in the reduction of NO by CO. They found that the reduction of NO by CO on α -MnO₂ proceeds by initially generating N₂O as an intermediate, which then dissociates into N₂ (Figure 4a). During the catalytic process, Mn²⁺ is easily oxidized to Mn³⁺, which can subsequently adsorb and dissociate NO, thus forming the intermediate N₂O. In situ investigations revealed the reconstruction of the α -MnO₂ surface, leading to the formation of a new active surface phase consisting of Mn³⁺ and OV_s serving as active sites. Among the various TiO₂-supported transition metal-based catalysts, MnO_x/TiO₂ shows the most promising CO-SCR activity at low temperatures. As illustrated in Figure 4b, the presence of NO on MnO_x/TiO₂ inhibits the oxidation of CO to CO₂. Instead, in situ Fourier transform infrared (FT-IR) studies found that the dissociation of NO takes place at the reduced Mn site, resulting in the generation of N₂O. N₂O acts as an intermediate and then reacts with CO to form N₂ [25].

When Mn in the Mn-based catalysts is present in a high valence state with numerous OV_s, it leads to an increased adsorption capacity for NO and CO. This condition also facilitates the occurrence of the L-H mechanism. In the L-H mechanism, the formation process of N₂O occurs as follows: NO and CO are adsorbed on the catalyst to form NO* and CO* (Equations (9) and (10)); then, NO* dissociated into N* and O* (Equation (11)). Subsequently, N* combines with another adsorbed NO to produce N₂O* (Equation (12)), which is further reduced by adsorbed CO to yield N₂ and CO₂ (Equation (13)):

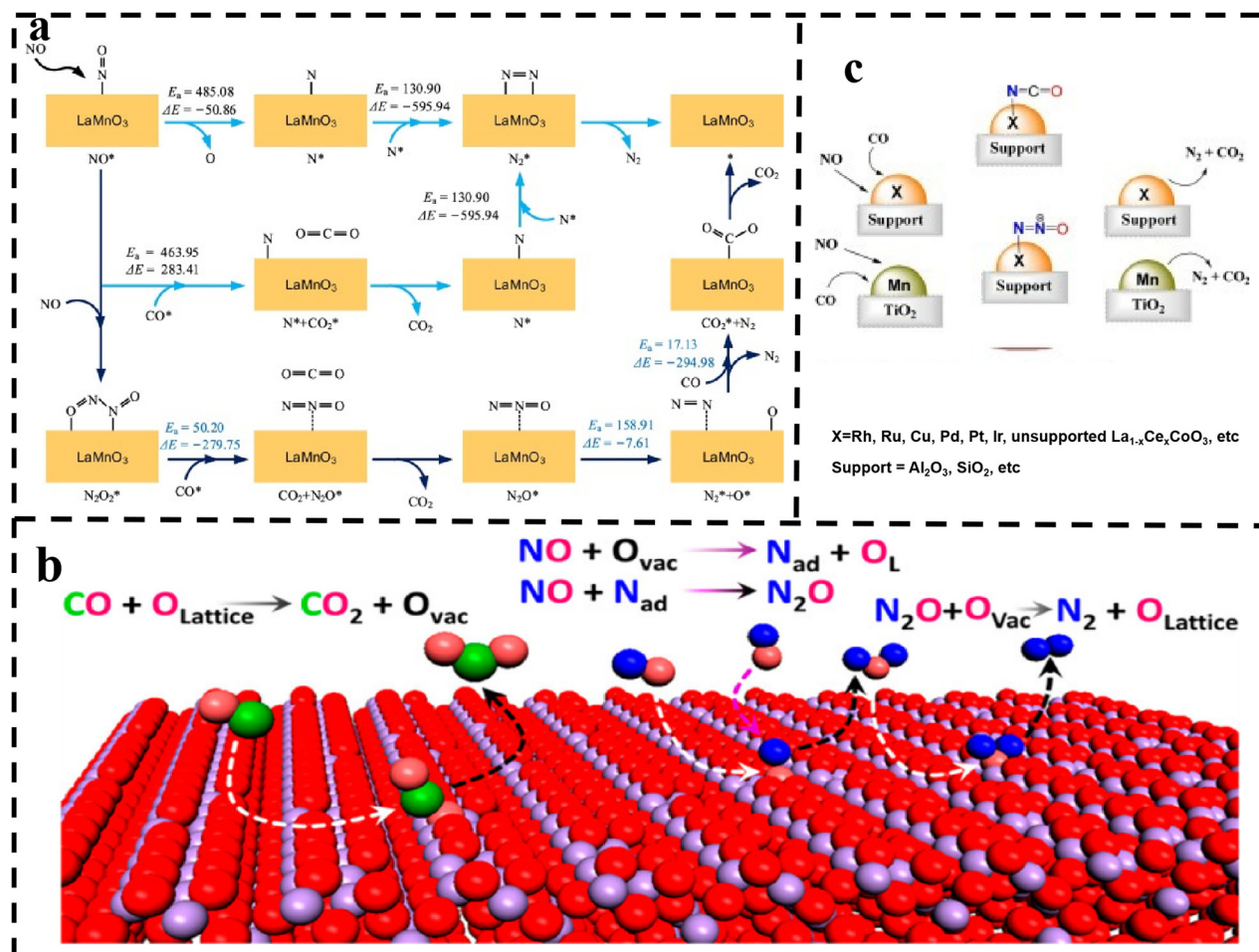
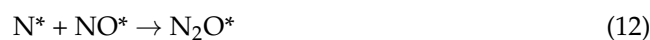
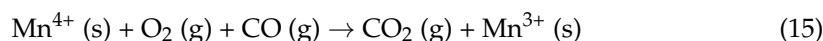
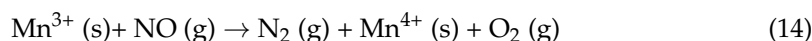


Figure 4. (a) Reaction mechanism on $\alpha\text{-MnO}_2$ nanorod catalyst [24]; (b) reaction mechanism on $\text{MnO}_x/\text{TiO}_2$ catalyst [25] (c) reaction mechanism on LaMnO_3 catalyst [58].

For the LaMnO_3 catalyst, the Mn site on its surface serves as the primary active site for NO reduction. In this case, N_2O_2^* generated through the NO coupling reaction acts as a crucial intermediate in the CO-SCR process. N_2O_2^* subsequently reacts with chemisorbed CO to produce CO_2 and N_2O^* intermediates. The reaction path of CO-SCR on the LaMnO_3 surface consists of three sequential steps: $2\text{NO}^* \rightarrow \text{N}_2\text{O}_2^*$, $\text{N}_2\text{O}_2^* + \text{CO}^* \rightarrow \text{N}_2\text{O}^* + \text{CO}_2$, and $\text{N}_2\text{O}^* + \text{CO}^* \rightarrow \text{N}_2 + \text{CO}_2^*$ (Figure 4c). The predominance of the bimolecular coupling mechanism in the CO-SCR reaction on the LaMnO_3 catalyst is attributed to the higher activation energy barrier for NO decomposition to N_2O on the LaMnO_3 surface compared to that of the N_2O_2^* formation [58]. In the case of the NiMn-MOF-74 catalyst, the in situ FT-IR results showed that NO molecules preferentially adsorbed on the catalyst surface and dissociated to N^* and O^* under the action of surface SSOVs. This process weakens the competitive adsorption of NO and CO on the catalyst. The dissociated NO undergoes subsequent reactions with CO to form N_2O intermediates, which are ultimately transformed into N_2 [31].

The presence of abundant variable valence states plays a crucial role in the catalytic activity and selectivity of Mn-based catalysts in the presence of oxygen. Mn^{3+} ions exhibit efficient adsorption and dissociation of NO. Lewis acid sites are very important for the CO-SCR reaction of MnO_x -based catalysts by enhancing the adsorption capability of CO molecules [41]. For the V_0 -OMS-2 catalyst, the reaction mechanism can be described as follows:



In summary, different Mn-based catalysts show different reaction mechanisms. When an N_2O intermediate is generated, the selectivity of the CO-SCR reaction may be compromised if N_2O , functioning as an intermediate, is unable to undergo further reduction by CO to form N_2 and CO_2 . Therefore, it is necessary to modify the composition, structure, oxidation state, and acid site of the Mn-based catalysts to facilitate the conversion of N_2O into N_2 . The diverse valence states of Mn play a crucial role in determining the catalytic activity and selectivity of the catalyst during the CO-SCR reaction. By adjusting the catalyst to achieve an appropriate oxidation state, it demonstrates improved resistance to oxygen.

5. Challenges

The concentrations of NO and CO in various industrial flue gases are different. Typically, the concentration of NO ranges between 500 ppm and 1600 ppm, whereas the CO concentration falls within the range of 1 vol% to 1.25 vol%. Besides CO and NO gases, there are also significant amounts of O_2 (≥ 5 vol%) and H_2O (≥ 10 vol%), as well as a minor quantity of SO_2 (≤ 50 ppm), which have a discernible impact on the catalytic activity of the catalyst in the CO-SCR reaction. For instance, an excess of oxygen may lead to favoring of the oxidation of CO and NO. SO_2 tends to form sulfates on the catalyst's surface, which can obstruct the surface active sites. H_2O can potentially compete with CO or NO for adsorption sites. On the other hand, the high catalytic activity required at low temperatures poses another challenge for the reaction. While the flue gas emission temperature in the power industry typically exceeds $350^\circ C$, most industrial furnaces operate at lower temperatures, with flue gas emissions ranging between 200 and $230^\circ C$. The flue gas temperature produced by industrial processes like steel sintering is typically below $150^\circ C$. Hence, the catalytic efficiency of the catalyst in the CO-SCR reaction at low temperatures is of significant importance. Although the precious metal catalysts described in the literature exhibit commendable catalytic activity under oxygen-rich conditions, their performance notably diminishes at lower temperatures. In contrast, low-cost Mn-based catalysts demonstrate significant potential in catalyzing the CO-SCR reaction at low temperatures (Table 2). Further investigation in this field is anticipated to result in the creation of catalysts capable of functioning at reduced reaction temperatures in oxygen-rich environments.

Table 2. Comparison of catalytic properties of Mn-based catalysts and other transition metal catalysts.

Catalyst	Gas Composition (%)					GHSV or WHSV	Temperature ($^\circ C$)	NO Conversion (%)	CO Conversion (%)	N_2 Selectivity (%)	Ref.
	NO	CO	O_2	SO_2	H_2O						
MnO_x/TiO_2	0.4	0.4	2.0	---	---	$50,000\ h^{-1}$	175	100	---	100	[29]
NiMn-MOF-74	0.5	1.0	---	0.1	5.0	$30,000\ h^{-1}$	200	100	---	---	[25]
Cu-Ce-Fe-Mn/ TiO_2	0.02	0.02	1.0	---	---	$10,000\ h^{-1}$	200	100	82	---	[28]
Mn-Ce O_2 @ Co_3O_4	1.0	2.0	5.0	0.05	10.0	$24,000\ h^{-1}$	200	82	100	78	[38]
$Mn_xCo_{3-x}O_4$	1.0	2.0	5.0	0.05	5.0	$20,000\ h^{-1}$	180	100	---	100	[37]
$Cu_{1.2}FeMg_{2.8}$ -LDO	0.03	0.12	1.0	0.05	5.0	$60,000\ mL\ g^{-1}h^{-1}$	225	100	---	100	[59]
Ce-Cu-BTC	0.1	0.1	5	---	---	---	300	100	70	100	[60]
CuO/TiO_2	1.0	1.0	0.5	---	---	$12,000\ h^{-1}$	250	100	---	90	[61]
NiFe/ CeO_2	0.05	0.5	0.5	---	---	$22,800\ h^{-1}$	250	100	---	100	[62]
Fe-Co/ASC	0.1	0.5	0.1	---	---	$20,000\ h^{-1}$	300	100	100	100	[63]
Fe@ CeO_2 -ZIF-8	0.5	0.1	---	---	5.0	$22,800\ h^{-1}$	300	100	50	99	[64]
Co_3O_4 - CeO_2 -IOV	0.1	0.2	5.0	0.05	10.0	$20,000\ h^{-1}$	200	100	100	100	[65]
Co SA + CoO_x NC/CZO	0.1	0.2	5.0	0.05	5.0	$20,000\ h^{-1}$	250	100	100	100	[12]

5.1. O₂

Due to the abundance of O₂, CO and NO may exhibit a preference for reacting with O₂. This can lead to enhanced CO consumption while preventing the reduction of NO to N₂. In particular, the hindrance of the CO-SCR reaction by an excess of O₂ (typically exceeding 5 vol.%) poses a significant challenge for the practical application of CO-SCR. On a Ni-Mn₂ catalyst, the presence of O₂ could inhibit the deNO_x process. Under the condition of a high O₂ concentration, part of NO could be converted to NO₂. Especially at high temperatures, the amount of NO₂ produced was greater than that of N₂, leading to the poor N₂ selectivity of the Ni-Mn₂ catalyst [66]. In the presence of 6% O₂, the CO conversion of the Mn-Ce-Fe-Co/TiO₂ catalyst reached 92%. Nevertheless, the NO conversion by Mn-Ce-Fe-Co/TiO₂ decreased as the O₂ content increased. This could be elucidated by the observation that in the presence of O₂, a portion of NO was oxidized to NO₂ instead of being converted to N₂, consequently leading to reduced NO_x conversion [34]. At an O₂ concentration of 8%, the NO conversion by a 5Fe-10Mn/AC catalyst was high in the reaction's early stages. However, its stability was notably poor, decreasing to 42% at 230 °C after only 7 min [67]. There are abundant variable valence states in Mn-based catalysts, and Mn³⁺ has been shown to be able to effectively adsorb and activate NO and strengthen N-O bond cleavage. Thus, regulating the valence state of Mn in Mn-based catalysts may be a solution to their poor catalytic activity and selectivity under oxygen-rich conditions.

Currently, it has been established that the dispersion of nanoparticles into single atoms (SAs) and the manipulation of the charge state of SAs can enhance the resistance of catalysts to O₂ in the CO-SCR reaction to a certain degree [9,10,68]. The underlying principle is that SACs possess an adaptable coordination structure, offering a favorable opportunity to modulate their catalytic efficacy [69]. Theoretically, Mn displays a wide range of variable valence states, and by adjusting the coordination environment of Mn SAs, distinct valence states of Mn can be achieved. The distinctive valence of Mn affects its adsorption capacity for reaction gases differently than that of O₂, potentially improving the O₂ resistance of Mn-based catalysts. While the utilization of Mn SAs in CO-SCR reactions has not been documented in the literature, studies have shown that Mn⁴⁺ in MnO₂ exhibits a higher affinity for NO compared to O₂, leading to a decrease in O₂ absorption [70]. Theoretically, the dispersion of Mn species in Mn-based catalysts into single atoms and the exposure of more Mn⁴⁺ species may enhance their O₂ resistance.

5.2. H₂O

In actual flue gas, a significant quantity of water is typically present. The presence of water will compete with NO for adsorption sites, leading to a reduction in NO conversion and N₂ selectivity [71]. However, the impact of water on the catalyst is reversible, and the catalyst can regain certain performance levels after the water is removed. For a CuMnO₂ nanosheet catalyst with the synergistic effect, it could achieve 100% NO conversion to N₂ at 310 °C. However, when 5% water vapor was introduced, the N₂ selectivity suddenly dropped from 90.2% to 10.1%, although the NO conversion increased from 89.2% to 100% (Figure 5a) [72]. When MnO_x was doped into CuO/CeO₂, the Cu/CeMn-10:1 catalyst (the molar ratio of CuO/CeO₂ to MnO_x was 10:1) showed the best catalytic activity in the NO + CO reaction, with 100% NO conversion and 83% N₂ selectivity at 220 °C in the absence of oxygen. After the introduction of 10 vol% H₂O into the reaction system, both the NO conversion and N₂ selectivity decreased, especially the N₂ selectivity [73]. The Mn-CeO₂@Co₃O₄ catalyst achieved 82% NO conversion and 78% N₂ selectivity at 200 °C with 5% O₂ present. When 10 vol.% H₂O was introduced, the NO conversion decreased to 65% (Figure 5b). The main reason for this decline was identified as the competitive adsorption of NO and H₂O [38].

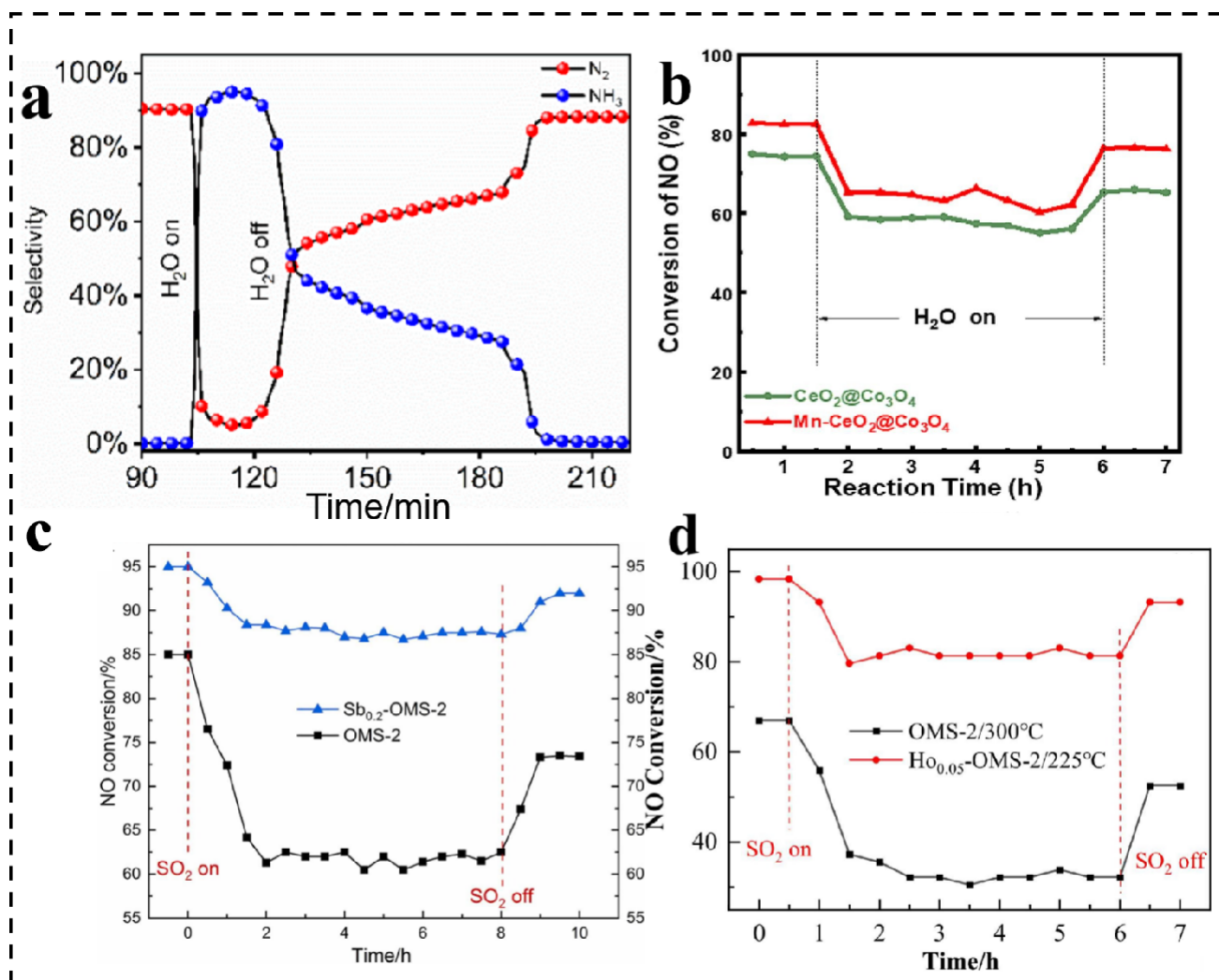


Figure 5. (a) N_2 and NH_3 selectivity of $CuMnO_2/SSM$ sample in the CO-SCR test under the conditions of 5% water, 1000 ppm NO, and 2000 ppm CO [72]; (b) effect of H_2O on NO conversion on $Mn-CeO_2@Co_3O_4$ catalyst activity at 200 °C [38]; (c) sulfur resistance stability test of $OMS-2$ and $Sb_{0.2}-OMS-2$ [42]; (d) influence of SO_2 on $Ho_{0.05}-OMS-2$ catalyst activity. Reaction conditions: NO = 0.05%, CO = 0.05%, O_2 = 2%, SO_2 = 0.02%, N_2 = balance, and GHSV = 15,000 h^{-1} [43].

5.3. SO_2

Small quantities of SO_2 are present in flue gas. In the case of Mn-based catalysts, their ability to tolerate sulfur is comparatively low. This is due to the formation of sulfides by SO_2 on the catalyst surface. In comparison to undoped $OMS-2$, an Sb-doped $Sb_{0.2}-OMS-2$ catalyst exhibited an increased proportion of OV on the catalyst surface and enriched Lewis acid sites, thus facilitating the conversion of NO. The NO conversion improved from 60% in $OMS-2$ to 83% in Sb-doped $Sb_{0.2}-OMS-2$ at 150 °C and from 80% to 95% at 300 °C. When SO_2 was introduced, the NO conversion of $OMS-2$ plummeted. While the introduction of Sb led to some improvement in sulfur resistance, the conversion of NO also showed a continuous decline, and the sulfur resistance was still limited (Figure 5c), which required further improvement [42]. Moreover, incorporating the metal Ho into $OMS-2$ also resulted in an enhancement in catalytic activity. Nonetheless, its resistance to sulfur was comparable to that of $Sb_{0.2}-OMS-2$ (Figure 5d) [43]. Likewise, the presence of SO_2 could have a substantial impact on the catalytic performance of $Mn-Ce-Fe-Co/TiO_2$ catalysts. When 50 ppm of SO_2 was introduced, the NO conversion of $Mn-Ce-Fe-Co/TiO_2$ experienced a notable decrease, with the lowest NO conversion being only 20% [34]. Indeed,

as mentioned above, the addition of metal can enhance sulfur resistance to some degree; however, there remains significant potential for further enhancement.

By coordinating with a low-electronegativity atom, the central atom acquires a negative charge, thereby enhancing the resistance to O₂ and SO₂ of the catalyst to some degree. This is based on the fact that the negatively charged single atom can boost the adsorption of NO while reducing the adsorption of O₂. Additionally, the adsorption capability of SO₂ is also diminished [9,69].

6. Conclusions and Perspectives

In recent years, CO-SCR technology has emerged as a prominent research focus in the denitrification field. Currently, the crucial aspect for the industrial implementation of CO-SCR technology lies in the development of cost-effective and high-performance catalysts. Mn-based catalysts offer advantages such as affordability and high activity at low temperatures. However, their development is hindered primarily by poor N₂ selectivity and stability in the presence of oxygen, as well as their limited water and sulfur resistance. In order to promote their industrialized application, it is crucial to tackle these issues. Subsequent research endeavors may be pursued with a focus on the following aspects:

(i) Presently, numerous studies have been published on SACs of precious metals, such as those based on Ir, Pd, and Pt. The dispersion of transition metals into single atoms to form effective catalysts has also been documented. For instance, a single-atom Mn catalyst has been utilized in various reactions such as oxygen reduction reactions [74] and the photocatalytic removal of water-based organics [75]. These reports provide support for the feasibility of synthesizing Mn SACs. However, currently, there is a lack of literature regarding the use of Mn SACs for the CO-SCR reaction. Previously, under the guidance of DFT, our research group successfully developed a catalyst consisting of Co SAs and CoO_x nanoclusters (NCs) with dual active centers co-anchored on the CZO support, which achieved superior catalytic performance at a broad temperature range between 250 and 400 °C and under 5 vol% O₂ conditions [12]. Therefore, by leveraging the benefits of the high low-temperature activity of Mn-based catalysts, there is the potential to obtain low-temperature performance. Furthermore, combining the Mn SAs with a support that possesses oxygen resistance may lead to outstanding low-temperature performance under oxygen-rich conditions.

(ii) Our group discovered that modifying the type and quantity of coordination atoms can alter their valence state in SACs. The adsorption behaviors of NO, CO, O₂, and SO₂ on negatively charged SACs significantly differ from those on positively charged SACs or nanoparticle catalysts [9,10]. For Mn-based catalysts, upon dispersing them into single atoms, the coordination type of the Mn atoms is adjusted to induce a negative charge, with the extent of negativity regulated by the quantity of coordinating atoms. By synthesizing negatively charged Mn SACs, it is possible to enhance their antioxidant properties and resistance to sulfur dioxide.

(iii) Various in situ characterization methods, such as in situ electron paramagnetic resonance (EPR), in situ transmission electron microscope (TEM), and in situ X-ray photoelectron spectroscopy (XPS), are frequently employed for defect identification of reaction intermediates and the changes in the structure and oxidation states of catalysts. Mn-based catalysts usually exhibit a significant number of defects, underscoring the critical necessity of accurately determining the defect type and density to gain insights into the underlying reaction mechanisms. Utilizing in situ techniques for observing the changes throughout the reaction process and integrating a variety of in situ characterization methods to thoroughly investigate the CO-SCR reaction process and elucidate the dynamic structure–activity relationship are crucial aspects. Hence, various in situ characterization techniques can be employed to observe reaction intermediates and clarify the reaction pathways for Mn-based catalysts, which is significant for designing more efficient Mn-based catalysts.

(iv) Our group employed solid-state ball milling technology to synthesize Co-based catalysts with excellent oxygen resistance and relatively high activity levels at low tem-

peratures [65]. The application of catalysts in industry necessitates simple preparation methods, superior catalytic performance, reproducibility, cost efficiency, and scalability for mass production. Hence, the development of straightforward, replicable, scalable, and promising preparation methodologies for Mn-based catalyst are imperative.

Author Contributions: D.L.: Writing—original draft, Visualization. M.C. and H.W.: Date curation. C.L. and B.L.: Resources. G.D. and S.H.: Software. Y.L.: Supervision. Y.J.: Writing—review and editing, Supervision, Visualization, Funding acquisition. All authors have read and agreed to the published version of the manuscript.

Funding: This research was funded by the National Natural Science Foundation of China grant number 21978299 from Y.J.; the Research Foundation for Advanced Talents of Beijing Technology and Business University grant number 19008020159 from Y.J.; the Graduate Research Ability Enhancement Program of Beijing Technology and Business University grant number 19008024042 from D.L.; and the Shccig-Qinling Program grant number SMYJY202400134C from Y.J.

Conflicts of Interest: The authors declare no competing interests.

References

1. Skalska, K.; Miller, J.S.; Ledakowicz, S. Trends in NO_x abatement: A review. *Sci. Total Environ.* **2010**, *408*, 3976–3989. [[CrossRef](#)] [[PubMed](#)]
2. Yun, L.; Li, Y.; Zhou, C.; Lan, L.; Zeng, M.; Mao, M.; Liu, H.; Zhao, X. The formation of CuO/OMS-2 nanocomposite leads to a significant improvement in catalytic performance for NO reduction by CO. *Appl. Catal. A Gen.* **2017**, *530*, 1–11.
3. Wang, C.; Wang, W.; Sardans, J.; An, W.; Zeng, C.; Abid, A.A.; Penuelas, J. Effect of simulated acid rain on CO₂, CH₄ and N₂O fluxes and rice productivity in a subtropical Chinese paddy field. *Environ. Pollut.* **2018**, *243*, 1196–1205. [[CrossRef](#)] [[PubMed](#)]
4. Andana, T.; Rappé, K.G.; Gao, F.; Szanyi, J.; Pereira-Hernandez, X.; Wang, Y. Recent advances in hybrid metal oxide-zeolite catalysts for low-temperature selective catalytic reduction of NO_x by ammonia. *Appl. Catal. B Environ.* **2021**, *291*, 120054. [[CrossRef](#)]
5. Inomata, Y.; Kubota, H.; Hata, S.; Kiyonaga, E.; Morita, K.; Yoshida, K.; Sakaguchi, N.; Toyao, T.; Shimizu, K.I.; Ishikawa, S.; et al. Tungsten-substituted vanadium oxide for low-temperature NO_x removal in the presence of water. *Nat. Commun.* **2021**, *12*, 557. [[CrossRef](#)] [[PubMed](#)]
6. Ren, D.; Gui, K.; Gu, S.; Wei, Y. Study of the nitric oxide reduction of SCR-NH₃ on γ-Fe₂O₃ catalyst surface with quantum chemistry. *Appl. Surf. Sci.* **2020**, *509*, 144659. [[CrossRef](#)]
7. Hu, Y.; Griffiths, K.; Norton, P.R. Surface science studies of selective catalytic reduction of NO: Progress in the last ten years. *Surf. Sci.* **2009**, *603*, 1740–1750. [[CrossRef](#)]
8. Jeon, J.; Ham, H.; Xing, F.; Nakaya, Y.; Shimizu, K.-i.; Furukawa, S. PdIn-Based Pseudo-Binary Alloy as a Catalyst for NO_x Removal under Lean Conditions. *ACS Catal.* **2020**, *10*, 11380–11384. [[CrossRef](#)]
9. Ji, Y.; Liu, S.; Song, S.; Xu, W.; Li, L.; Zhang, Y.; Chen, W.; Li, H.; Jiang, J.; Zhu, T.; et al. Negatively Charged Single-Atom Pt Catalyst Shows Superior SO₂ Tolerance in NO_x Reduction by CO. *ACS Catal.* **2023**, *13*, 224–236. [[CrossRef](#)]
10. Ji, Y.; Liu, S.; Zhu, H.; Xu, W.; Jiang, R.; Zhang, Y.; Yu, J.; Chen, W.; Jia, L.; Jiang, J.; et al. Isolating Contiguous Ir Atoms and Forming Ir-W Intermetallics with Negatively Charged Ir for Efficient NO Reduction by CO. *Adv. Mater.* **2022**, *34*, 2205703. [[CrossRef](#)]
11. Hungría, A.B.; Fernández-García, M.; Anderson, J.A.; Martínez-Arias, A. The effect of Ni in Pd-Ni/(Ce, Zr)O_x/Al₂O₃ catalysts used for stoichiometric CO and NO elimination. Part 2: Catalytic activity and in situ spectroscopic studies. *J. Catal.* **2005**, *235*, 262–271. [[CrossRef](#)]
12. Liu, S.; Ji, Y.; Liu, B.; Xu, W.; Chen, W.; Yu, J.; Zhong, Z.; Xu, G.; Zhu, T.; Su, F. Co Single Atoms and CoO_x Nanoclusters Anchored on Ce_{0.75}Zr_{0.25}O₂ Synergistically Boosts the NO Reduction by CO. *Adv. Funct. Mater.* **2023**, *33*, 2303297. [[CrossRef](#)]
13. He, J.; Kang, R.; Wei, X.; Huang, J.; Feng, B.; Nam Hui, K.; San Hui, K.; Wu, D. Comparative study of MCo_{0.75}Zr_{0.25}O_y (M = Cu, Mn, Fe) catalysts for selective reduction of NO by CO: Activity and reaction pathways. *Carbon Resour. Convers.* **2021**, *4*, 205–213. [[CrossRef](#)]
14. Wang, X.; Li, X.; Mu, J.; Fan, S.; Wang, L.; Gan, G.; Qin, M.; Li, J.; Li, Z.; Zhang, D. Facile Design of Highly Effective CuCe_xCo_{1-x}O_y Catalysts with Diverse Surface/Interface Structures toward NO Reduction by CO at Low Temperatures. *Ind. Eng. Chem. Res.* **2019**, *58*, 15459–15469. [[CrossRef](#)]
15. Hamada, H.; Haneda, M. A review of selective catalytic reduction of nitrogen oxides with hydrogen and carbon monoxide. *Appl. Catal. A Gen.* **2012**, *421*, 1–13. [[CrossRef](#)]
16. Wang, J.; Gao, F.; Dang, P.; Tang, X.; Lu, M.; Du, Y.; Zhou, Y.; Yi, H.; Duan, E. Recent advances in NO reduction with CO over copper-based catalysts: Reaction mechanisms, optimization strategies, and anti-inactivation measures. *Chem. Eng. J.* **2022**, *450*, 137374. [[CrossRef](#)]
17. Chen, X.; Liu, Y.; Liu, Y.; Lian, D.; Chen, M.; Ji, Y.; Xing, L.; Wu, K.; Liu, S. Recent Advances of Cu-Based Catalysts for NO Reduction by CO under O₂-Containing Conditions. *Catalysts* **2022**, *12*, 1402. [[CrossRef](#)]

18. Liu, S.; Gao, J.; Xu, W.; Ji, Y.; Zhu, T.; Xu, G.; Zhong, Z.; Su, F. A review of the catalysts used in the reduction of NO by CO for gas purification. *Chem. Eng. J.* **2024**, *486*, 150285. [[CrossRef](#)]
19. Wang, Y.; Xu, W.; Liu, H.; Chen, W.; Zhu, T. Catalytic removal of gaseous pollutant NO using CO: Catalyst structure and reaction mechanism. *Environ. Res.* **2024**, *246*, 150285. [[CrossRef](#)]
20. Gholami, Z.; Luo, G.; Gholami, F.; Yang, F. Recent advances in selective catalytic reduction of NO_x by carbon monoxide for flue gas cleaning process: A review. *Environ. Sci. Pollut. Res.* **2021**, *63*, 68–119. [[CrossRef](#)]
21. Li, S.; Wang, F.; Ng, D.; Shen, B.; Xie, Z. Stability challenges and prospects for the industrial application of non-noble catalysts for selective catalytic reduction of NO_x by CO (CO-SCR). *ChemCatChem* **2024**, *16*, e202301246. [[CrossRef](#)]
22. Xie, J.; Fang, D.; He, F.; Chen, J.; Fu, Z.; Chen, X. Performance and mechanism about MnO_x species included in MnO_x/TiO₂ catalysts for SCR at low temperature. *Catal. Commun.* **2012**, *28*, 77–81. [[CrossRef](#)]
23. Jin, Q.; Han, L.; Li, N.; Zhang, T.; Gao, E.; Yao, M.; Yao, S.; Wu, Z.; Li, J.; Zhu, J.; et al. Exploring the influence of chemical state of Cu species on CO-SCR performance in spinel-type CuM₂O₄ (M = Co, Mn, Fe, Ni, and Cr): The synergy between Cu²⁺ and surface oxygen vacancy. *Fuel* **2024**, *360*, 130553. [[CrossRef](#)]
24. Shan, J.; Zhu, Y.; Zhang, S.; Zhu, T.; Rouvimov, S.; Tao, F. Catalytic Performance and in Situ Surface Chemistry of Pure α-MnO₂ Nanorods in Selective Reduction of NO and N₂O with CO. *J. Phy. Chem. C* **2013**, *117*, 8329–8335. [[CrossRef](#)]
25. Boningari, T.; Pavani, S.M.; Ettireddy, P.R.; Chuang, S.S.C.; Smirniotis, P.G. Mechanistic investigations on NO reduction with CO over Mn/TiO₂ catalyst at low temperatures. *Mol. Catal.* **2018**, *451*, 33–42. [[CrossRef](#)]
26. Zhang, L.; Li, B.; Liu, C.; Tian, H.; Hong, M.; Yin, X.; Feng, X. NO reduction with CO over a highly dispersed Mn/TiO₂ catalyst at low temperature: A combined experimental and theoretical study. *Nanotechnology* **2021**, *32*, 505717. [[CrossRef](#)] [[PubMed](#)]
27. Sreekanth, P.M.; Smirniotis, P.G. Selective reduction of NO with CO over titania supported transition metal oxide catalysts. *Catal. Lett.* **2008**, *122*, 37–42. [[CrossRef](#)]
28. Zhang, Y.; Zhao, L.; Chen, Z.; Li, X. Promotional effect for SCR of NO with CO over MnO_x-doped Fe₃O₄ nanoparticles derived from metal-organic frameworks. *Chin. J. Chem. Eng.* **2022**, *46*, 113–125. [[CrossRef](#)]
29. Liu, T.; Yao, Y.; Wei, L.; Shi, Z.; Han, L.; Yuan, H.; Li, B.; Dong, L.; Wang, F.; Sun, C. Preparation and Evaluation of Copper Manganese Oxide as a High-Efficiency Catalyst for CO Oxidation and NO Reduction by CO. *J. Phy. Chem. C* **2017**, *121*, 12757–12770. [[CrossRef](#)]
30. Li, D.; Yu, Q.; Li, S.-S.; Wan, H.-Q.; Liu, L.-J.; Qi, L.; Liu, B.; Gao, F.; Dong, L.; Chen, Y. The Remarkable Enhancement of CO-Pretreated CuO-Mn₂O₃/γ-Al₂O₃ Supported Catalyst for the Reduction of NO with CO: The Formation of Surface Synergetic Oxygen Vacancy. *Chem. Eur. J.* **2011**, *17*, 5668–5679. [[CrossRef](#)]
31. Shi, Y.; Chu, Q.; Xiong, W.; Gao, J.; Huang, L.; Zhang, Y.; Ding, Y. A new type bimetallic NiMn-MOF-74 as an efficient low-temperatures catalyst for selective catalytic reduction of NO by CO. *Chem. Eng. Process.* **2021**, *159*, 108232. [[CrossRef](#)]
32. Li, L.; Wang, Y.; Zhang, L.; Yu, Y.; He, H. Low-Temperature Selective Catalytic Reduction of NO_x on MnO₂ Octahedral Molecular Sieves (OMS-2) Doped with Co. *Catalysts* **2020**, *10*, 396. [[CrossRef](#)]
33. Fan, F.; Wang, L.; Wang, L.; Liu, J.; Wang, M. Low-Temperature Selective NO Reduction by CO over Copper-Manganese Oxide Spinels. *Catalysts* **2022**, *12*, 591. [[CrossRef](#)]
34. Pan, K.L.; Young, C.W.; Pan, G.T.; Chang, M.B. Catalytic reduction of NO by CO with Cu-based and Mn-based catalysts. *Catal. Today* **2020**, *348*, 15–25. [[CrossRef](#)]
35. Shi, X.; Chu, B.; Wang, F.; Wei, X.; Teng, L.; Fan, M.; Li, B.; Dong, L.; Dong, L. Mn-Modified CuO, CuFe₂O₄, and γ-Fe₂O₃ Three-Phase Strong Synergistic Coexistence Catalyst System for NO Reduction by CO with a Wider Active Window. *ACS Appl. Mater. Int.* **2018**, *10*, 40509–40522. [[CrossRef](#)] [[PubMed](#)]
36. Wang, J.; Xing, Y.; Su, W.; Li, K.; Zhang, W. Bifunctional Mn-Cu-CeO_x/γ-Al₂O₃ catalysts for low-temperature simultaneous removal of NO_x and CO. *Fuel* **2022**, *321*, 124050. [[CrossRef](#)]
37. Gholami, F.; Gholami, Z.; Tomas, M.; Vavrunkova, V.; Mirzaei, S.; Vakili, M. Promotional Effect of Manganese on Selective Catalytic Reduction of NO by CO in the Presence of Excess O₂ over M@La-Fe/AC (M = Mn, Ce) Catalyst. *Catalysts* **2020**, *10*, 1322. [[CrossRef](#)]
38. Meng, Y.; Liu, S.; Wang, Y.; Xu, W.; Gao, J.; Yu, S.; Su, F.; Zhu, T. Hollow Mn-doped CeO₂@Co₃O₄ catalyst for NO reduction by CO. *J. Catal.* **2024**, *430*, 115311. [[CrossRef](#)]
39. Li, X.; Ren, S.; Chen, Z.; Wang, M.; Chen, L.; Chen, H.; Yin, X. A Review of Mn-Based Catalysts for Abating NO_x and CO in Low-Temperature Flue Gas: Performance and Mechanisms. *Molecules* **2023**, *28*, 6885. [[CrossRef](#)]
40. Wei, L.; Liu, T.; Wu, Y.; Liu, H.; Dong, L.; Li, B. Design of co-symbiotic Fe_xMn_yO catalysts for NO reduction by CO. *Catal. Sci. Technol.* **2020**, *10*, 7894–7903. [[CrossRef](#)]
41. He, H.; Wang, Y.; Fu, W.; Zhang, L.; Zeng, J.; Zhu, G. Study on the CO-SCR anti-sulfur and denitration performance of V-doped OMS-2 catalysts. *Ceram. Inter.* **2021**, *47*, 33120–33126. [[CrossRef](#)]
42. Wang, Y.; Zhang, C.; Zhang, L.; Zeng, J.; He, H. Anti-sulfur selective catalytic reduction of NO_x on Sb-doped OMS-2. *Appl. Catal. A Gen.* **2022**, *641*, 118684. [[CrossRef](#)]
43. Luo, B.; Wang, Z.; Huang, J.; Ning, S.; Deng, W.; Zhao, B.; Su, Y. Study on CO-SCR denitrification performance of Ho-modified OMS-2 catalyst. *J. Environ. Chem. Eng.* **2023**, *11*, 119050. [[CrossRef](#)]
44. Yao, X.; Xiong, Y.; Sun, J.; Gao, F.; Deng, Y.; Tang, C.; Dong, L. Influence of MnO₂ modification methods on the catalytic performance of CuO/CeO₂ for NO reduction by CO. *J. Rare Earths* **2014**, *32*, 131–138. [[CrossRef](#)]

45. Deng, C.S.; Qian, J.N.; Yu, C.X.; Yi, Y.N.; Zhang, P.; Li, W.; Dong, L.H.; Li, B.; Fan, M.G. Influences of doping and thermal stability on the catalytic performance of CuO/Ce₂₀M₁O_x (M = Zr, Cr, Mn, Fe, Co, Sn) catalysts for NO reduction by CO. *Rsc. Adv.* **2016**, *6*, 113630–113647. [[CrossRef](#)]
46. Liu, S.; Ji, Y.; Xu, W.; Zhang, J.; Jiang, R.; Li, L.; Jia, L.; Zhong, Z.; Xu, G.; Zhu, T.; et al. Hierarchically interconnected porous Mn_xCo_{3-x}O₄ spinels for low-temperature catalytic reduction of NO by CO. *J. Catal.* **2022**, *406*, 72–86. [[CrossRef](#)]
47. Wan, H.; Li, D.; Dai, Y.; Hu, Y.; Liu, B.; Dong, L. Catalytic behaviors of CuO supported on Mn₂O₃ modified γ -Al₂O₃ for NO reduction by CO. *J. Mol. Catal. A Chem.* **2010**, *332*, 32–44. [[CrossRef](#)]
48. Li, C.; Shi, Y.; Zhao, Q.D.; Xiong, W.; Ding, Y.; Sun, J.H.; Huang, Y.L.; Zhao, Z.F. A stable spherical MOF-derived Mn_x-Fe₂O₃/C catalysts for low-temperature CO-SCR. *Chem. Eng. J.* **2023**, *475*, 146388. [[CrossRef](#)]
49. Liu, T.; Wei, L.; Yao, Y.; Dong, L.; Li, B. La promoted CuO-MnO_x catalysts for optimizing SCR performance of NO with CO. *Appl. Surf. Sci.* **2021**, *546*, 148971. [[CrossRef](#)]
50. Wang, L.; Cheng, X.; Wang, Z.; Ma, C.; Qin, Y. Investigation on Fe-Co binary metal oxides supported on activated semi-coke for NO reduction by CO. *Appl. Catal. B Environ.* **2017**, *201*, 636–651. [[CrossRef](#)]
51. Huang, B.-f.; Wang, D.-f.; Li, J.-l.; Shi, Z. Cu-Fe/activated carbon catalyst for low-temperature CO-selective catalytic: Modification and denitration mechanism. *Environ. Prog. Sustain. Energy* **2022**, *41*, e13827. [[CrossRef](#)]
52. Li, J.; Zhu, J.; Fu, S.; Tao, L.; Chu, B.; Qin, Q.; Wang, J.; Li, B.; Dong, L. Insight into copper-cerium catalysts with different Cu valence states for CO-SCR and in-situ DRIFTS study on reaction mechanism. *Fuel* **2023**, *339*, 126962. [[CrossRef](#)]
53. Sun, Y.; Wu, Y.; Bai, Y.; Wu, X.; Wang, H.; Wu, Z. High performance iridium loaded on natural halloysite nanotubes for CO-SCR reaction. *Fuel* **2024**, *357*, 129938. [[CrossRef](#)]
54. Tao, L.; Wang, J.; Qin, Q.; Chu, B.; Gao, P.; Qiu, J.; Li, Q.; Du, X.; Dong, L.; Li, B. Simple anion-modified layered double oxides use for controlling Cu valence states for low-temperature CO-SCR. *Surf. Interfaces* **2024**, *44*, 103654. [[CrossRef](#)]
55. Li, W.; Liu, Z.; Yu, F.; Pan, K.; Zhao, H.; Gao, F.; Zhou, M.; Dai, B.; Dan, J. CuCeO_x/VMT powder and monolithic catalyst for CO-selective catalytic reduction of NO with CO. *New J. Chem.* **2022**, *46*, 10422–10432. [[CrossRef](#)]
56. Du, Y.; Gao, F.; Tang, X.; Yi, H.; Zhou, Y.; Zhao, S.; Duan, E.; Wang, J.; Qi, Z. Mechanistic insight into the enhanced NO reduction by CO over a pre-reduced Cu_xO_y-CeO₂ multiphase catalyst. *J. Environ. Chem. Eng.* **2023**, *11*, 110386. [[CrossRef](#)]
57. Liu, T.; Qian, J.; Yao, Y.; Shi, Z.; Han, L.; Liang, C.; Li, B.; Dong, L.; Fan, M.; Zhang, L. Research on SCR of NO with CO over the Cu_{0.1}La_{0.1}Ce_{0.8}O mixed-oxide catalysts: Effect of the grinding. *Mol. Catal.* **2017**, *430*, 43–53. [[CrossRef](#)]
58. Yan, X.; Liu, J.; Yang, Y.; Wang, Z.; Zheng, Y. A catalytic reaction scheme for NO reduction by CO over Mn-terminated LaMnO₃ perovskite: A DFT study. *Fuel Process. Technol.* **2021**, *216*, 106798. [[CrossRef](#)]
59. Liu, J.; Zang, P.; Liu, X.; Mi, J.; Wang, Y.; Zhang, G.; Chen, J.; Zhang, Y.; Li, J. A novel highly active catalyst form CuFeMg layered double oxides for the selective catalytic reduction of NO by CO. *Fuel* **2022**, *317*, 123469. [[CrossRef](#)]
60. Zhang, Y.; Zhao, L.; Duan, J.; Bi, S. Insights into deNO_x processing over Ce-modified Cu-BTC catalysts for the CO-SCR reaction at low temperature by in situ DRIFTS. *Sep. Purif. Technol.* **2020**, *234*, 116081. [[CrossRef](#)]
61. Amano, F.; Suzuki, S.; Yamamoto, T.; Tanaka, T. One-electron reducibility of isolated copper oxide on alumina for selective NO-CO reaction. *Appl. Catal. B Environ.* **2006**, *64*, 282–289. [[CrossRef](#)]
62. Li, S.; Chen, X.; Wang, F.; Xie, Z.; Hao, Z.; Liu, L.; Shen, B. Promotion effect of Ni doping on the oxygen resistance property of Fe/CeO₂ catalyst for CO-SCR reaction: Activity test and mechanism investigation. *J. Hazard. Mater.* **2022**, *431*, 128622. [[CrossRef](#)] [[PubMed](#)]
63. Cheng, X.; Wang, L.; Wang, Z.; Zhang, M.; Ma, C. Catalytic Performance of NO Reduction by CO over Activated Semicoke Supported Fe/Co Catalysts. *Ind. Eng. Chem. Res.* **2016**, *55*, 12710–12722. [[CrossRef](#)]
64. Li, S.; Wang, F.; Xie, Z.; Ng, D.; Shen, B. A novel core-shell structured Fe@CeO₂-ZIF-8 catalyst for the reduction of NO by CO. *J. Catal.* **2023**, *421*, 240–251. [[CrossRef](#)]
65. Liu, S.; Xue, W.; Ji, Y.; Xu, W.; Chen, W.; Jia, L.; Zhu, T.; Zhong, Z.; Xu, G.; Mei, D.; et al. Interfacial oxygen vacancies at Co₃O₄-CeO₂ heterointerfaces boost the catalytic reduction of NO by CO in the presence of O₂. *Appl. Catal. B Environ.* **2023**, *323*, 122151. [[CrossRef](#)]
66. Sun, P.; Li, X.; Cheng, X.; Wang, Z.; Wang, P. Transition metal modified Mn-based catalysts for CO-SCR in the presence of excess oxygen. *Process Saf. Environ. Protect.* **2023**, *176*, 389–401. [[CrossRef](#)]
67. Huang, B.; Shi, Z.; Yang, Z.; Dai, M.; Wen, Z.; Li, W.; Zi, G.; Luo, L. Mechanism of CO selective catalytic reduction denitration on Fe-Mn/AC catalysts at medium and low temperatures under oxygen atmosphere. *Chem. Eng. J.* **2022**, *446*, 137412. [[CrossRef](#)]
68. Ji, Y.; Chen, X.; Liu, S.; Song, S.; Xu, W.; Jiang, R.; Chen, W.; Li, H.; Zhu, T.; Li, Z.; et al. Tailoring the Electronic Structure of Single Ag Atoms in Ag/WO₃ for Efficient NO Reduction by CO in the Presence of O₂. *ACS Catal.* **2023**, *13*, 1230–1239. [[CrossRef](#)]
69. Zhang, X.; Gao, D.; Zhu, B.; Cheng, B.; Yu, J.; Yu, H. Enhancing photocatalytic H₂O₂ production with Au co-catalysts through electronic structure modification. *Nat. Commun.* **2024**, *15*, 3212. [[CrossRef](#)]
70. Li, H.; Wang, D.; Hui, S. Adsorption of NO and O₂ on MnO₂ and (MnO₂)₃/Al₂O₃. *Appl. Surf. Sci.* **2021**, *569*, 150994. [[CrossRef](#)]
71. Xia, Z.; Zhang, R.; Duan, J.; Liu, Y.; Li, Z.; Gou, X. Performance of Mn-Ce-Fe/FA Catalysts on Selective Catalytic Reduction of NO_x with CO under Different Atmospheres. *Energies* **2023**, *16*, 3859. [[CrossRef](#)]
72. Yang, Y.; Yang, L.; Cao, G.; Cui, Y.; Feng, L.; Jia, L.; Zhang, X.; Li, J.; Liu, B. Monolithic CuMnO₂-Nanosheet-Based Catalysts In Situ Grown on Stainless Steel Mesh for Selective Catalytic Reduction of NO with CO. *ACS Appl. Nano Mater.* **2023**, *6*, 4803–4811. [[CrossRef](#)]

73. Deng, C.; Huang, Q.; Zhu, X.; Hu, Q.; Su, W.; Qian, J.; Dong, L.; Li, B.; Fan, M.; Liang, C. The influence of Mn-doped CeO₂ on the activity of CuO/CeO₂ in CO oxidation and NO plus CO model reaction. *Appl. Surf. Sci.* **2016**, *389*, 1033–1049. [[CrossRef](#)]
74. Li, Y.; Li, Z.; Shi, K.; Luo, L.; Jiang, H.; He, Y.; Zhao, Y.; He, J.; Lin, L.; Sun, Z.; et al. Single-Atom Mn Catalysts via Integration with Mn Sub Nano-Clusters Synergistically Enhance Oxygen Reduction Reaction. *Small* **2024**, *20*, 2309727. [[CrossRef](#)]
75. Wang, J.; Xu, Z.; Xu, Y.; Liu, S.; Qiu, J.; Wang, Z.; Wang, Y.; Weng, Y.; Cao, H.; Wang, S.; et al. Mn single atoms for one-electron photoozonation of aqueous organics. *Appl. Catal. B Environ. Energy* **2024**, *349*, 123900. [[CrossRef](#)]

Disclaimer/Publisher's Note: The statements, opinions and data contained in all publications are solely those of the individual author(s) and contributor(s) and not of MDPI and/or the editor(s). MDPI and/or the editor(s) disclaim responsibility for any injury to people or property resulting from any ideas, methods, instructions or products referred to in the content.